ISSN: 2664-9640

New Type of Stack Temperature Field Measurement System for SOFC

Hao Bai, Xin Wu

School of energy power and mechanical engineering, North China Electric Power University, Beijing 102206, China

Abstract

Solid Oxide Fuel Cell (SOFC) has the advantages of high efficiency and cleanness, and its reverse process can be used for hydrogen production by solid oxide electrolytic cell, which is a major research focus of new energy technology. However, the working performance of SOFC stack is affected by temperature, and the abnormal working temperature will directly affect the performance and life of the battery pack. Therefore, it is of great significance for the stable, efficient and long-term operation of SOFC stack to obtain the temperature field distribution and then monitor the maximum temperature and maximum temperature gradient inside the stack. Firstly, the SOFC stack temperature field measurement system is designed and built based on the fiber array composed of several quartz optical fiber sensors and the rectangular coordinate manipulator. The developed system can measure the temperature in multiple gas channels of the stack at the same time. Then, according to the size characteristics of SOFC stack cathode airway, the quintic polynomial trajectory planning method based on intermediate variables is proposed to reduce the vibration of the manipulator when it holds probes and make them move at the uniform speed in gas channels. Finally, the effectiveness of the stack temperature field measurement system is verified through experiments. The developed measurement system can provide technical support for the construction of the internal temperature field of the stack.

Keywords

Solid oxide fuel cell; stack temperature field measurement system; fiber array; trajectory planning.

1. Introduction

Solid oxide fuel cell (SOFC) is a power generation device that can directly use hydrogen, methanol and other fuels to generate electricity. Through wind-hydrogen coupled power generation, wind power drives solid oxide electrolysis cells to electrolyze water to produce hydrogen, which provides fuel for solid oxide fuel cells, and can also effectively solve the volatility and randomness problems of wind power generation[1,2]. Solid oxide fuel cells do not have problems such as electrolyte corrosion, and do not require noble metals as catalysts. It can directly convert the chemical energy of fuel into electrical energy, and has the advantages of high efficiency and cleanliness, so it has broad application prospects[3,4]. The operating temperature of solid oxide fuel cells is relatively high, usually above 600 degrees Celsius[5]. Due to the uneven temperature distribution inside the fuel cell, the thermal expansion coefficient of each component is different, resulting in thermal stress inside the fuel cell, which exceeds the capacity of the stack material. When subjected to the limit, the stack structure will be damaged. In order to widely apply solid oxide fuel cells, it is urgent to solve the problems of production cost, safety and reliability of fuel cells. Temperature is an important parameter that affects the service life and working performance of solid oxide fuel cells. When the stack temperature is lower than the working temperature, the stack cannot reach the normal working state, and the

ISSN: 2664-9640

electrical performance output capability decreases; when the temperature exceeds the normal working temperature, the durability of the material Insufficient, will reduce the operating life of the stack[6]. According to the literature[7,8], although the temperature distribution of the fuel cell is uneven, the temperature change is not large, and the working life of the stack will not be affected when the temperature difference does not exceed 10K/cm. Therefore, the accurate acquisition of the stack temperature field distribution of the solid oxide fuel cell can further improve its working performance and prolong its service life. The working characteristics of solid oxide fuel cells are very complex, and their performance is affected by multiphysics in the form of strong coupling. At present, most studies on SOFC stack temperature use modeling and simulation methods to simplify the fuel cell model to solve the temperature field distribution in the stack. The obtained results have a large deviation from the actual[9,10] The purpose of this paper is to design a new type of stack temperature field measurement system for SOFC.

2. SOFC stack temperature field measurement system

Most of the existing studies on the actual temperature measurement of SOFC stacks use thermocouples as temperature sensors. Wilkinson[11]embedded 19 micro-thermocouples on the anode plate and the cathode plate respectively. Due to the fragility of the micro-thermocouples, only 10 thermocouples were finally able to collect data. Mench[12]placed 8 R-type thermocouples between the electrolyte materials, and only 3 thermocouples measured the temperature due to the damage of the thermocouples in the process of making the membrane electrode assembly or the battery assembly process.

In the non-contact temperature measurement method, infrared temperature measurement uses the relationship between the temperature and its radiation intensity to convert the optical signal into an electrical signal that can be processed. By analyzing the relationship between the electrical signal and the radiation intensity, the measured For the temperature information of the object, although the infrared imaging thermometry method has high spatial resolution, it can only reveal the temperature distribution on the surface of the stack[13], and cannot measure the temperature inside the stack. Professor Liu Wenzhong's team[14,15]calculated the temperature to be measured based on the Langevin function according to the magnetization of magnetic nanoparticles at different temperatures, and the measurement error can be less than 0.1K.

As shown in the structure diagram of SOFC stack as shown in Fig. 1, a large number of cathode gas channels are distributed on each layer of cells, and the size of the gas channels is only about 1 mm. According to the actual temperature measurement method of the stack, the micro temperature sensor is installed in the fuel cell, which can Used to measure the temperature at a single point of the fuel cell. However, this measurement method increases the difficulty of sealing the fuel cell, and the sensor may be damaged during the actual operation, so that the measurement cannot be performed. Such sensors are affected by the performance of response time, spatial resolution and measurement accuracy, so it is difficult to quickly establish the stack temperature field.

Although the thermocouple can accurately obtain the temperature value of the measurement point[16], there is a big difference between the parameter values of the fuel cell reaction area, which cannot reflect the real temperature distribution inside the stack, and cannot replace the battery by several temperature measurement points. The real state of the internal electrochemical reaction zone[17]cannot accurately measure the temperature change inside the battery in real time. By increasing the number of thermocouples, it will not only increase the measurement cost, but also weaken the sealing performance of the stack and limit its large-scale application. The existing non-contact temperature measurement methods and infrared temperature measurement methods can only measure the surface temperature of the fuel cell,

ISSN: 2664-9640

but cannot measure the internal temperature of the stack; the magnetic nanometer temperature measurement method is difficult to apply to the temperature measurement of the stack temperature field with complex internal structure. Therefore, the above temperature measurement methods cannot meet the measurement requirements of the stack temperature field.

In view of the shortcomings of the above temperature measurement methods, this paper designs and builds a new SOFC stack temperature field measurement system based on a fiber array composed of silica fiber sensors with higher performance in response time and measurement accuracy, and a Cartesian coordinate manipulator. According to the size characteristics of the cathode gas channel of SOFC stack, a quintic polynomial trajectory planning method based on intermediate variables is proposed, which reduces the jitter when the probe is clamped by the Cartesian coordinate manipulator and ensures that the probe runs at a uniform speed in the cathode gas channel. Finally, through experiments, the effectiveness of the proposed stack temperature field measurement system is verified.

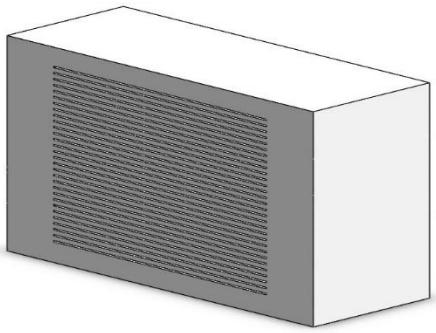

Fig.1 SOFC stack structure diagram

2.1. Silica fiber temperature sensor

According to the size characteristics of the stack cathode gas channel of the solid oxide fuel cell and the shortcomings of the existing fuel cell temperature measurement methods, this paper uses a quartz fiber temperature sensor from a domestic company as shown in Fig. 2 to measure the internal temperature of the stack cathode gas channel. This sensor is based on the principle of black body radiation for temperature measurement. The diameter of the quartz fiber probe used in the sensor is 0.4 mm. Compared with thermocouples, the quartz fiber probe is non-conductive, free from electromagnetic interference, and has a response time of less than 400 ms, which is more suitable for Temperature measurement inside a solid oxide fuel cell. The fuel cell stack is composed of multiple single cells, and a large number of air passages are distributed on each cell. In order to improve the temperature measurement efficiency, several optical fiber probes are used to form an optical fiber array, and multiple air passages are measured at the same time. During temperature measurement, the quartz fiber probe transmits the thermal radiation emitted by the stack to the rear temperature processing unit. The temperature processing unit obtains the temperature value according to the functional relationship between the thermal radiation intensity and the temperature, and uses the multi-channel data acquisition card to collect and save it to in the computer.

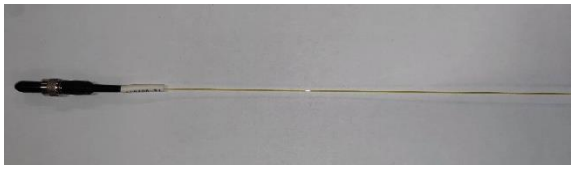

Fig.2 Optical fiber temperature sensor probe

ISSN: 2664-9640

2.2. Cartesian coordinate manipulator

When using the optical fiber probe to measure the temperature at various points inside the stack, it is necessary to ensure that it can run stably and uniformly in the cathode gas channel. Considering the structure of the cathode gas channel of the stack, the movement of the optical fiber probe can be realized by the Cartesian coordinate manipulator. In order to obtain the temperature field distribution of the stack, a Cartesian coordinate manipulator as shown in Fig. 3 is used to clamp the fiber probe. The manipulator is driven by a stepping motor, and a grating ruler is installed on the x, y, and z coordinate axes of the manipulator. When measuring the temperature, the rectangular coordinate manipulator clamps a fiber array composed of multiple probes and inserts it at the outlet end of the cathode gas channel, and the position of the fiber array is obtained through the grating ruler on each coordinate axis of the manipulator, and finally the temperature field distribution map of the stack can be drawn. Thus, the stack temperature field measurement is completed.

Fig. 3 Physical drawing of rectangular coordinate manipulator

2.3. Cartesian coordinate manipulator trajectory planning method

Because the probe is long, the jitter generated by the manipulator during operation will be amplified at the end of the probe. When the vibration is too large, the probe will collide with the stack and break, which will affect the temperature measurement. Therefore, it is necessary to plan the trajectory of the manipulator reasonably, reduce the shaking of the manipulator, and improve the stability of the manipulator. Trajectory planning is to give speed and acceleration information to the trajectory of the manipulator, and obtain the functional relationship between the position of the end of the manipulator and time. The goal of trajectory planning is that the manipulator can run quickly, accurately and smoothly. It also requires the manipulator to approach the target point quickly without producing significant impact, and to have a smooth trajectory during operation, keeping the speed and acceleration continuous. Commonly used trajectory planning methods include polynomial interpolation and spline function interpolation. The cubic polynomial velocity curve can remain continuous, but the acceleration curve is discontinuous at the start and end points. The quintic polynomial can not only ensure the continuity of the velocity and acceleration curves, but also obtain an ideal trajectory planning effect. The functional relationship between the manipulator's trajectory and time is established in the polynomial trajectory planning, which can ensure the continuity of the manipulator's position and speed. There is no sudden change in speed and acceleration during the process.

Considering the advantages and disadvantages of polynomial trajectory planning and the need for the manipulator to grip the probe, the speed and acceleration of the manipulator should transition smoothly, and the maximum jerk of the manipulator motion should be as small as possible. The smooth acceleration corresponds to the third derivative of the manipulator motion. The curve should be kept continuous to avoid the vibration of the manipulator caused

ISSN: 2664-9640

by the sudden acceleration of acceleration, and the jerk at the beginning and end of the manipulator movement should be zero. The trajectory of a Cartesian manipulator can be described by a series of intervals, and the trajectory planning based on the intermediate variable u is applied to each interval, and the quintic polynomial coefficients are determined according to the constraints of the start and end points[18].

r(u) is used to represent the motion function of the displacement of each axis of the Cartesian coordinate manipulator with respect to the intermediate variable *u* during the movement of the manipulator, and the position, velocity and acceleration of the starting point and end point of the manipulator in the kth interval are given, and the fifth time of the trajectory of the k^{th} interval is given. The polynomial is represented as follows:

$$r(u)_{k\to k+1} = C_0 + C_1 \cdot u + C_2 \cdot u^2 + C_3 \cdot u^3 + C_4 \cdot u^4 + C_5 \cdot u^5 \tag{1}$$

The quintic polynomial contains six coefficients. In order to determine the trajectory of the manipulator, six constraints are required, two of which are the position of the manipulator corresponding to the known start and end times, the other two conditions are the speed of the manipulator at the start and end times, and the last two The first condition is the acceleration of the manipulator at the start and end time. Formula (1) is derived and substituted into the constraints:

$$\begin{cases} r_0 = C_0 \\ r_f = C_0 + C_1 \cdot u + C_2 \cdot u^2 + C_3 \cdot u^3 + C_4 \cdot u^4 + C_5 \cdot u^5 \\ \dot{r_0} = C_1 \\ \dot{r_f} = C_1 + 2 \cdot C_2 \cdot u + 3 \cdot C_3 \cdot u^2 + 4 \cdot C_4 \cdot u^3 + 5 \cdot C_5 \cdot u^4 \\ \ddot{r_0} = 2 \cdot C_2 \\ \ddot{r_f} = 2 \cdot C_2 + 6 \cdot C_3 \cdot u + 12 \cdot C_4 \cdot u^2 + 20 \cdot C_5 \cdot u^3 \end{cases} \tag{2}$$

The running speed of the manipulator along the space trajectory can be expressed by the differential of displacement to time[19]:

$$v(t) = \left|\frac{ds}{dt}\right| = \left|\frac{ds}{du} \cdot \frac{du}{dt}\right| \tag{3}$$

where $\frac{du}{dt} = \frac{v(t)}{\sqrt{(x\prime)^2+(y\prime)^2+(z\prime)^2}}$; $\frac{ds}{du} = \sqrt{(x')^2 + (y')^2 + (z')^2}$; $x' = dx/du$; $y' = dy/du$; $z' = dz/du$.

where *u* is a function as time *t*. From the current parameter u_i and the first and second derivatives of *u* to time *t*, the Taylor expansion is used to find the parameter u_{i+1} as follows:

$$u_{i+1} = u_i + T_i \cdot \dot{u_i} + (T_i^2/2) \cdot \ddot{u_i} + o(T_i) \tag{4}$$

where $i = 1\cdots N$; $T_i = t_{i+1} - t_i$; $\dot{u_i} = \frac{du_i}{dt} = \frac{v(t)}{\sqrt{[x(i)']^2+[y(i)']^2+[z(i)']^2}}$;

$$\ddot{u_i} = \frac{dv(t)}{dt}\frac{1}{\sqrt{[x(i)]^2+[y(i)]^2+[z(i)']^2}} - \frac{v(t)^2\cdot[x(i)'\cdot x(i)''+y(i)'\cdot y(i)''+z(i)'\cdot z(i)'']}{\{[x(i)']^2+[y(i)']^2+[z(i)']^2\}^2}$$

w is a general variable representing the *x*, *y*, and *z* axes. The formulas for the speed, acceleration and jerk of the manipulator are as follows:

$$\begin{cases} v(w) = w(u)' \cdot \dot{u_i} \\ a(w) = w(u)'' \cdot \dot{u_i}^2 + w(u)' \cdot \ddot{u_i} \\ J(w) = w(u)^{(3)} \cdot \dot{u_i}^3 + 3 \cdot w(u)'' \cdot \dot{u_i} \cdot \ddot{u_i} \end{cases} \tag{5}$$

ISSN: 2664-9640

3. SOFC stack temperature field measurement system verification

Firstly, the positioning accuracy experiment of rectangular coordinate manipulator is carried out, and the trajectory parameters obtained by quintic polynomial trajectory planning are input into the manipulator control system. In order to verify the accuracy of manipulator, the starting point of manipulator is set as (0,0,0) mm and the end point is set as (40,40,110) mm. The size of the cathode airway of SOFC stack measured in this paper is about 1mm. In order to prevent the probe from breaking due to collision with the stack when the probe moves, set the maximum deviation range of the manipulator to 0.05mm, the uniform speed to v_{max} = 2mm/s, and the maximum acceleration a_{max} = 3mm/s^2. The actual operation track and position deviation are shown in Fig. 4. The position deviation is calculated as follows:

$$\delta = \sqrt{(x - x_{act})^2 + (y - y_{act})^2 + (z - z_{act})^2} \tag{6}$$

where x, y and z are the planning coordinates of the manipulator; x_{act}, y_{act} and z_{act} are grating rulers to measure the actual position of the manipulator.

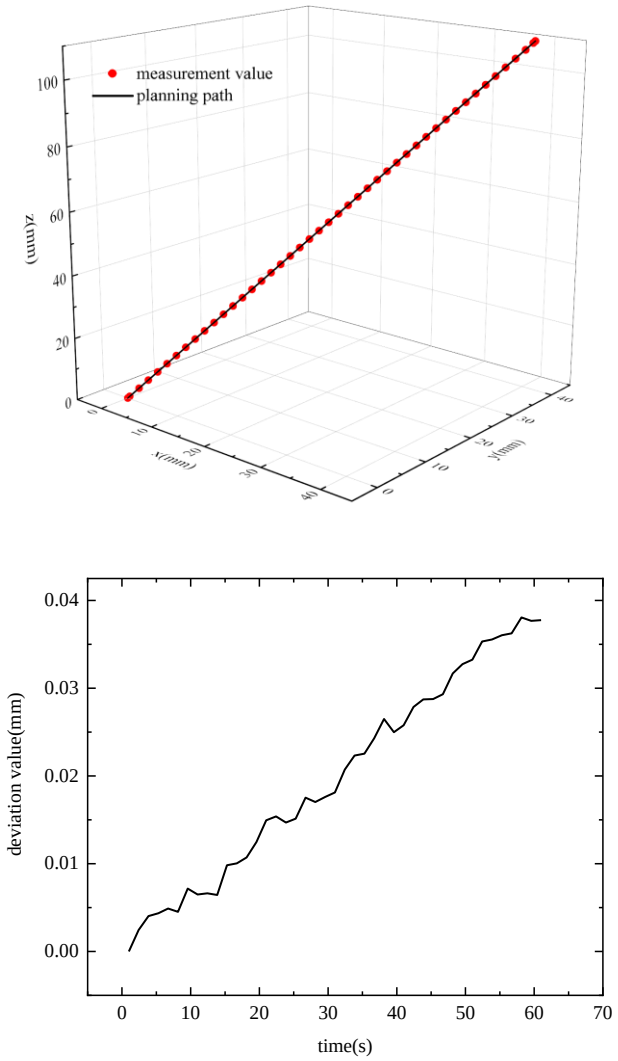

Fig. 4 Actual trajectory and deviation diagram

As shown in Fig. 4, the trajectory and trajectory deviation of the manipulator are shown. The displacement deviation of the manipulator is within 0.05 mm, which meets the requirements of positioning accuracy. As shown in Fig. 5 and Fig. 6, during the actual operation of the

ISSN: 2664-9640

manipulator, the speed and acceleration remain continuous. Therefore, the designed Cartesian coordinate manipulator trajectory planning method can meet the proposed positioning accuracy and jitter suppression requirements.

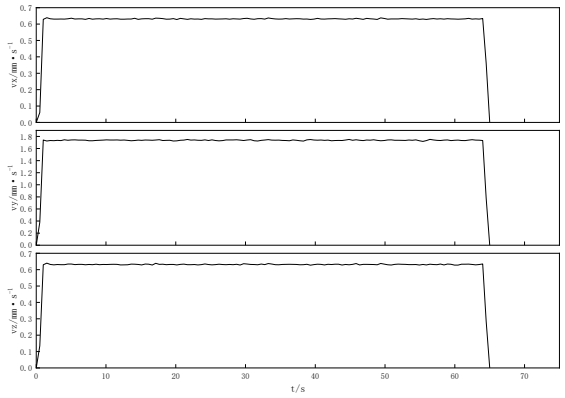

Fig. 5 Actual running speed diagram

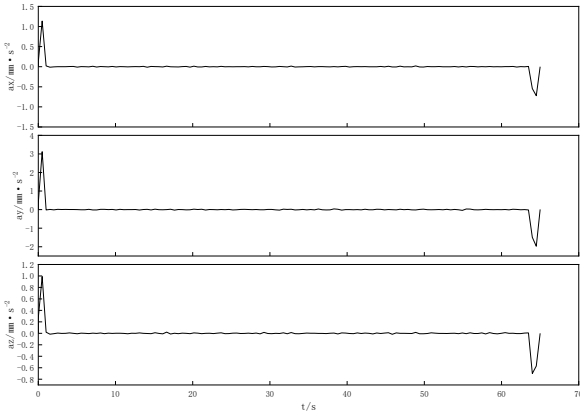

Fig. 6 Actual running acceleration diagram

Fig. 7 Stack temperature field measurement diagram

ISSN: 2664-9640

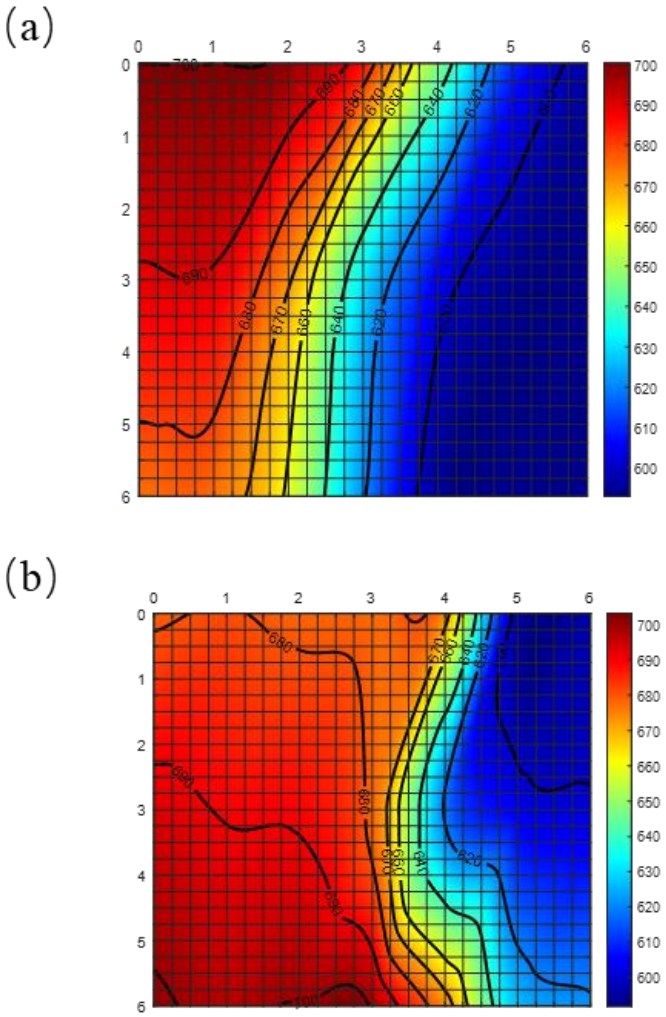

Fig. 8 Measured temperature field diagram of gas channels: (a) measure airway temperature field 1 (b) measures airway temperature field 2

In the stack temperature field measurement system shown in Fig. 7, a clamping device is used to connect an optical fiber array consisting of two optical fiber probes to the end effector of the manipulator, and a ceramic tube is protected outside the optical fiber probe. A heating furnace is built using a heat preservation board and a heating plate, the stack model is placed in the heating furnace, a hole is made on the side of the heating furnace so that the probe can be inserted into the cathode gas channel, the heating temperature is set to 700 °C, and the optical fiber is clamped by a Cartesian coordinate manipulator.The array moves in the direction of gas inlet to outlet in the stack cathode gas channel, and temperature measurement at each point is carried out.

Two-dimensional interpolation is performed on the temperature measurement data obtained by each fiber optic probe to obtain the temperature field map of the measured airway as shown in Fig. 8. As shown in Fig. 8, the temperature in the cathode gas channel from the gas inlet to the outlet gradually decreases, which is in line with the actual situation. Therefore, the measurement system designed and constructed in this paper can meet the measurement requirements of SOFC stack temperature field.

4. Summary

In view of the shortcomings of the current SOFC stack temperature field measurement methods, this paper proposes a new SOFC stack temperature field measurement system.

ISSN: 2664-9640

The proposed stack temperature field measurement system uses a quartz fiber temperature sensor for temperature measurement, uses a Cartesian coordinate manipulator to clamp an optical fiber array composed of multiple probes, and applies a quintic polynomial trajectory planning method based on intermediate variables. Suppress the vibration of the probe during operation, and ensure that the probe runs at a uniform speed in the airway.

In the experiment, the displacement, velocity and acceleration of the manipulator in the actual operation process all meet the set requirements, and the temperature measurement data also meet the actual situation, which verifies the effectiveness of the proposed stack temperature field measurement system. Provided technical support.

References

[1] DENG H,CHEN J,TENG Y,et al. Research on energy management strategy of wind hydrogen coupling system［J］. Journal of Solar Energy,Vol. 42(2021):256-263.

[2] CAI G W,XI Y F,YANG D Y,et al. Economic performance analysis of gas electric heating combined system model based on wind hydrogen［J］. Journal of solar energy,Vol. 40(2019):1465-1471.

[3] TAN Y. Study on new oxygen electrode for solid oxide electrolytic cell[D]. Huazhong University of science and technology,2016.

[4] PENG S P,HAN M F,YANG C B,et al. Solid oxide fuel cell[J]. Physics,Vol. 02(2004):90-94.

[5] SONG S D,HAN M F,SUN Z H. Research progress of solid oxide fuel cell flat panel stack［J］. Science Bulletin,Vol. 59(2014):1405-1416.

[6] WU X D. Study on two-dimensional temperature distribution estimation of application-oriented flat plate cross flow SOFC stack[D]. Huazhong University of science and technology,2019.

[7] AGUIAR P,ADJIMAN C S,BRANDON N P. Anode-supported intermediate temperature direct internal reforming solid oxide fuel cell. I:model-based steady-state performance［J]. Journal of Power Sources,Vol. 138(2004):120-136.

[8] ZHAO W Q,JIANG J H,QIN H C,et al. Machine learning based soft sensor and long-term calibration scheme:A solid oxide fuel cell system case［J］. International Journal of Hydrogen Energy, Vol. 46(2021):17322-17342.

[9] PARK J,KANG J,BAE J. Computational analysis of operating temperature,hydrogen flow rate and anode thickness in anode-supported flat-tube solid oxide fuel cells［J］. Renewable Energy, Vol. 54(2013):63-69.

[10] MANGLIK Raj M,MAGAR Yogesh N. Heat and Mass Transfer in Planar Anode-Supported Solid Oxide Fuel Cells:Effects of Interconnect Fuel/Oxidant Channel Flow Cross Section［J］. Journal of Thermal Science and Engineering Applications,Vol. 7(2015):041003-1-10.

[11] WILKINSON M,BLANCO M,Gu E,et al. In situ experimental technique for measurement of temperature and current distribution in proton exchange membrane fuel cells［J］. Electrochemical and Solid State Letters,Vol. 9(2006):A507-A511.

[12] MENCH M M,BURFORD D J,DAVIS T W. In situ temperature distribution measurement in an operating polymer electrolyte fuel cell[C]//ASME International Mechanical Engineering Congress and Exposition. Vol.37181(2003):415-428.

[13] SAUNDERS J E A,DAVY M H. In-situ studies of gas phase composition and anode surface temperature through a model DIR-SOFC steam–methane reformer at 973. 15 K［J］. International Journal of Hydrogen Energy,Vol. 38(2013):13762-13773.

[14] ZHONG J,LIU W,ZHOU M,et al. AC magnetization measurement employing a pair of differentiating coils for magnetic nanoparticle noninvasive and remote temperature estimation[C]//2012 IEEE

ISSN: 2664-9640

International Instrumentation and Measurement Technology Conference Proceedings. IEEE,2012:1780-1783.

[15] XIANG Q,ZHONG J,ZHOU M,et al. AC field dependence of cluster disruption in magnetic fluids [J]. Journal of Applied Physics,Vol. 109(2011): 07B317.

[16] NIE Z H,GUO H,YE F,et al. Progress of contact measurement technology for internal temperature of fuel cell [J]. Modern Chemical Industry,Vol. 31 (2011):17-22.

[17] LEE C Y,HSIEH W J,WU G W. Embedded flexible micro-sensors in MEA for measuring temperature and humidity in a micro-fuel cell [J]. Journal of Power Sources, Vol. 181(2008):237-243.

[18] LIN R S,KOREN Y. Ruled surface machining on five-axis CNC machine tools [J]. Journal of Manufacturing Processes,Vol. 2(2000):25-35.

[19] WU X,LI Y Y,LIU S,et al.Local minimum-time trajectory planning for five-axis machining with and without tool tip deviation [J].International Journal of Mechatronics and Manufacturing Systems,Vol. 4(2011): 304-321.